N89-29888

7.2 SMALL-SCALE STRUCTURE AND TURBULENCE OBSERVED IN MAP/WINE

T. A. Blix

Norwegian Defence Research Establishment
P. O. Box 25
N-2007 Kjeller, Norway

During MAP/WINE small-scale structure and turbulence in the mesosphere and lower thermosphere was studied *in situ* by rocket-borne instruments as well as from the ground by remote sensing techniques. The eight salvoes launched during the campaign resulted in a wealth of information on the dynamical structure of these regions. The paper reviews the experimental results and discusses their interpretation in terms of gravity waves and turbulence. It is shown that eddy diffusion coefficients and turbulent energy dissipation rates may be derived from the *in situ* measurements in a consistent manner. The observations are also shown to be consistent with the hypothesis that turbulence can be created by a process of gravity wave saturation.

DERIVATION OF ε AND K

(A) CONSERVATION OF ENERGY (THRANE ET AL, 1985)

(B) STRUCTURE FUNCTION (HOCKING, 1985; TATARSKII, 1961, 1971)

THE STRUCTURE FUNCTION CONSTANT C_E^2 IS GIVEN BY:

$$C_E^2 = a^2 N \varepsilon^{-1/3} \quad \text{AND} \quad N = K_E \left[\left[\frac{\partial E}{\partial x}\right]^2 + \left[\frac{\partial E}{\partial y}\right]^2 + \left[\frac{\partial E}{\partial z}\right]^2 \right] = K_E \beta M_E^2$$

WHERE:

$$M_E = \frac{\partial E}{\partial z}$$

FROM THE EQUATIONS ABOVE ONE CAN OBTAIN (HOCKING, 1985; BLIX, 1988):

$$\varepsilon = \left[a^2 \alpha' R_i \beta\right]^{-3/2} \left[C_E^2\right]^{3/2} \omega_B^3 M_E^3$$

CRITICAL QUESTIONS:

(1) WHAT IS THE RICHARDSON NUMBER ?

HOCKING (1985): $R_i = R_i(\text{crit.}) = 0.25$
WEINSTOCK (1978): $R_i = 0.8$

(2) IS THERE ANY RELATION BETWEEN VARIATIONS IN THE VERTICAL AND HORIZONTAL DIRECTION ?

HOCKING (1985): $\partial E/\partial x = \partial E/\partial y = 0$
BLIX (1988): $\partial E/\partial x = \partial E/\partial y = \partial E/\partial z$

Figure 1. Procedure for deriving turbulence parameters. Good agreement between the two models (A and B) is obtained using $R_i = 0.8$ instead of 0.25, and $\frac{\partial}{\partial x} = \frac{\partial}{\partial y} = \frac{\partial}{\partial z}$ instead of $\frac{\partial}{\partial x} = \frac{\partial}{\partial y} = 0$.

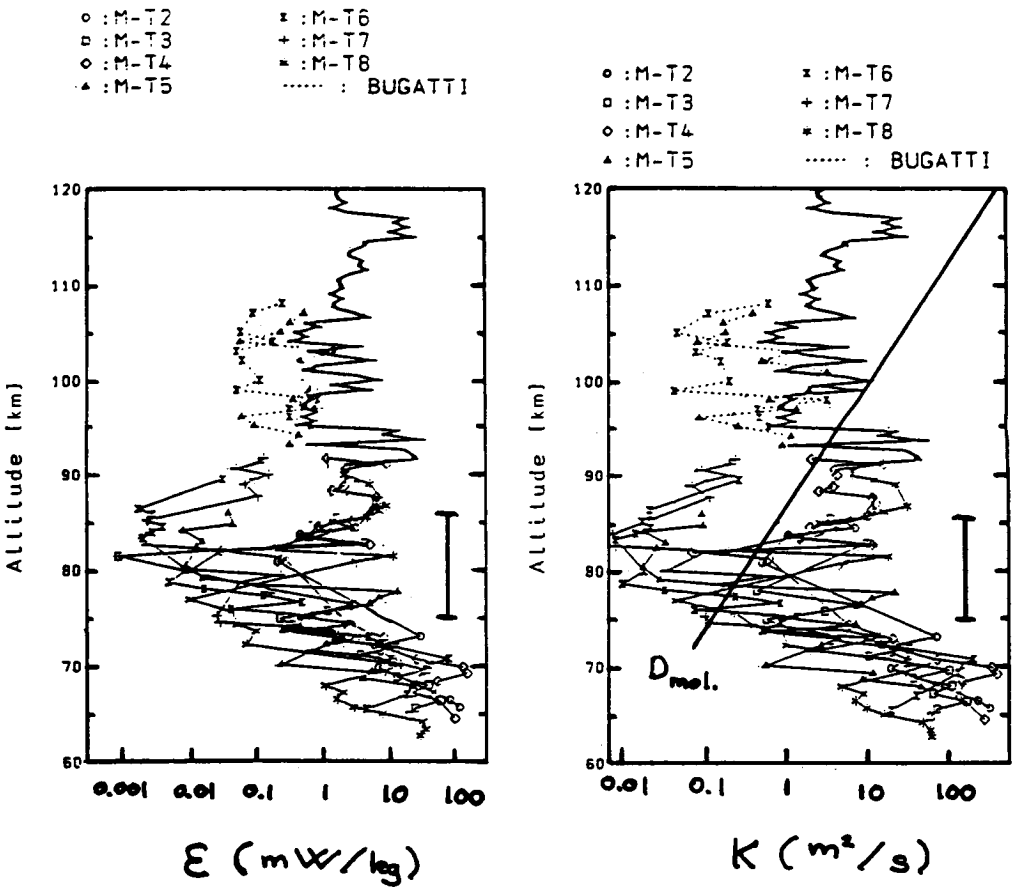

Figure 2. ε and K derived from the PIP and BUGATTI flights. Energy dissipation rates ε (left panel) and eddy diffusion coefficients K (right panel) derived from the positive ion probe (PIP) and the BUGATTI mass spectrometer flown during MAP/WINE. Note the minimum in turbulence activity at or below the mesopause region (vertical bars in the figure).

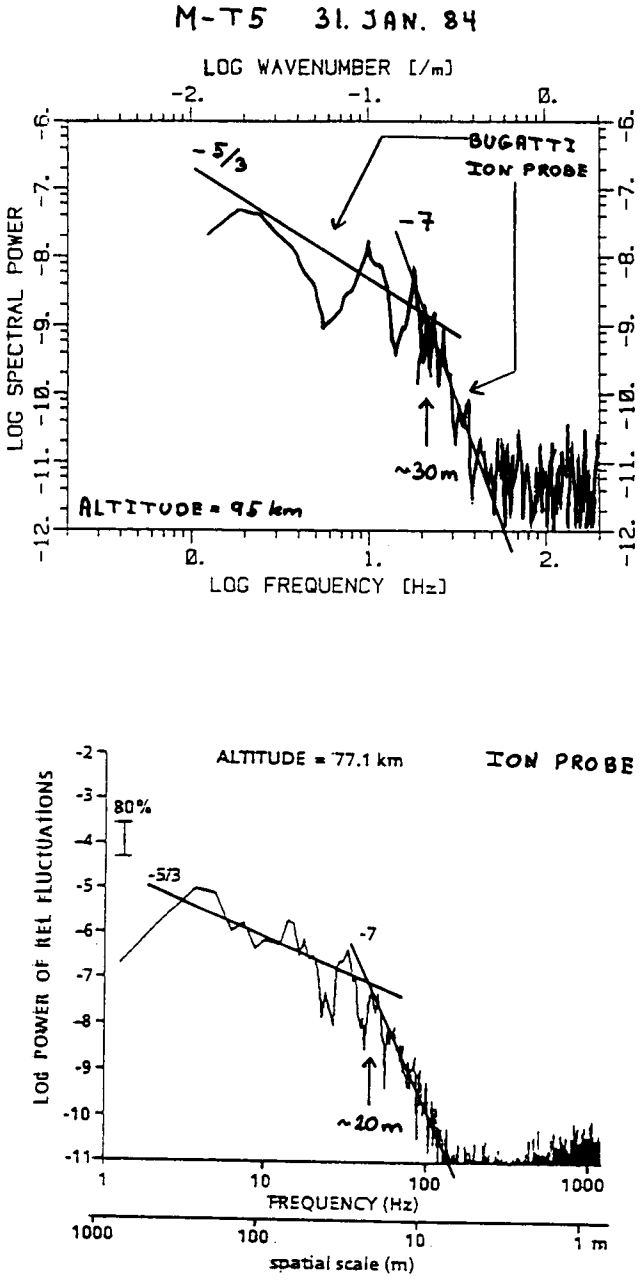

Figure 3. Upper panel: Comparison of spectra at neutral density fluctuations observed with the positive ion probe and the BUGATTI mass spectrometer during flight M-T5 31 Jan 84 at 95 km height. Note break in spectrum from –5/3 to –7 at a scale of about 30 m. Lower panel: Spectrum of ion density fluctuations observed with the positive ion probe during flight M-T5 31 Jan 1984 at 77 km height. Note break in spectrum from –5/3 to –7 at a scale of about 20 m.

TYPICAL SCALES OF THE OBSERVED TURBULENCE

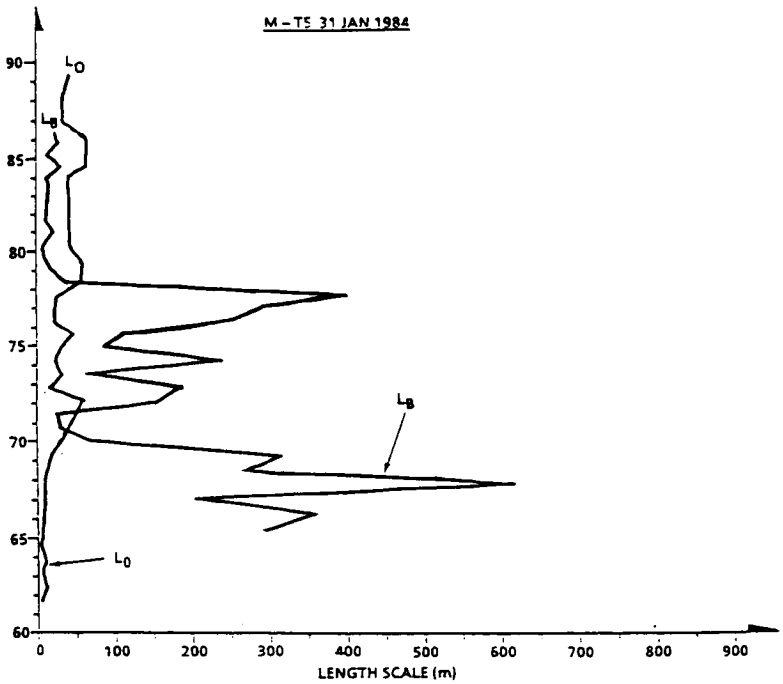

$$L_B = \left[0.271\, M_{\frac{\Delta n}{n}}^{2}\right]^{-3/4} \left[C_{\frac{\Delta n}{n}}^{2}\right]^{3/4}$$

$$M_{\frac{\Delta n}{n}} = \left[\frac{1}{H_n} - \frac{1}{\gamma H_p}\right]$$

Figure 4. Transition scale L_0 (break in spectral slope from 5/3 to –7) and buoyancy length scale L_B (derived from the formula shown) versus height from the M-T5 flight 31 Jan 1984.

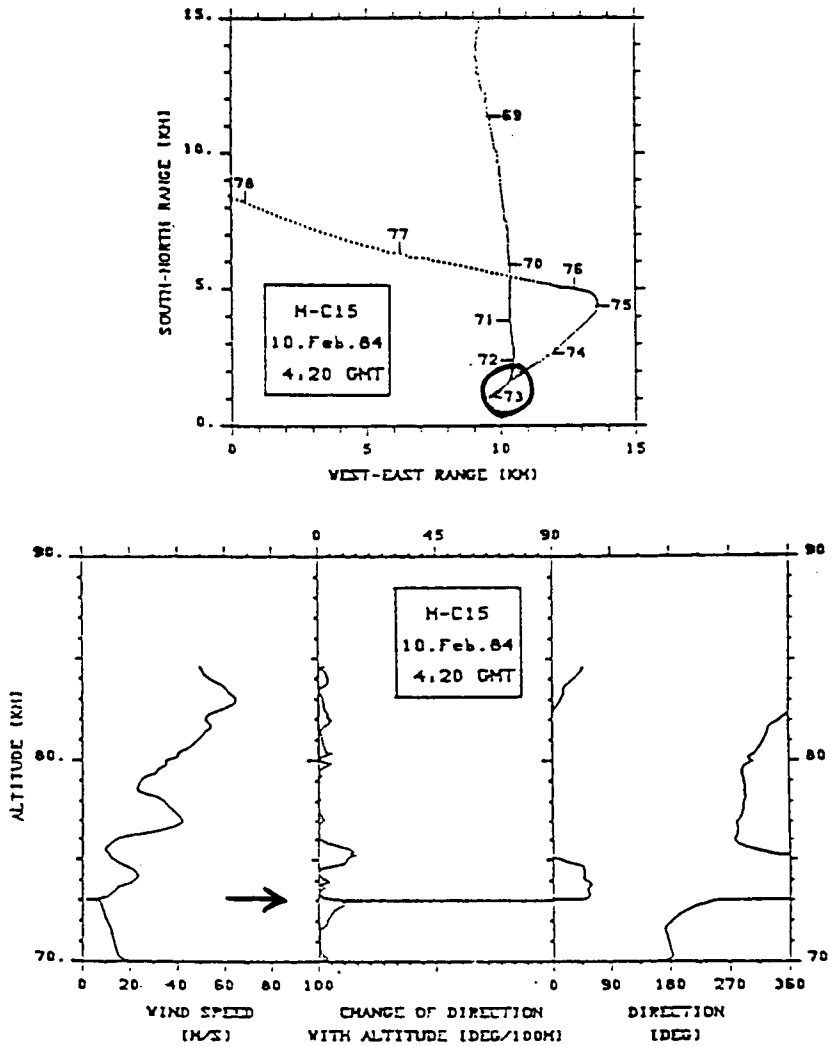

HIGH LATITUDE (69°N) WINTER

Figure 5. Typical wind corner observed with the foil cloud (chaff) M-C15 on Feb 10 1984. Wind corner at 73 km height is characterized by a minimum in wind speed associated with a sharp change in wind direction with height.

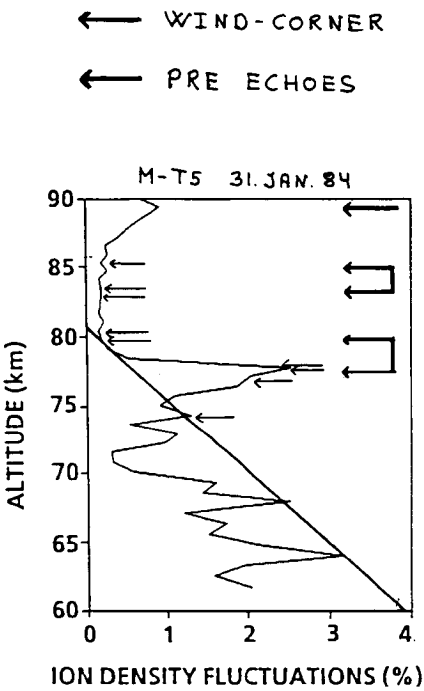

Figure 6. An example showing the correlation between ion density fluctuations (solid curve), wind corners (light arrows) and PRE echoes (heavy arrows). The heavy sloping line is the minimum intensity of ion density fluctuations that can be observed by PRE for normal noise intensity.

	PRE ECHOES	ION DENSITY FLUCTUATIONS	WIND CORNERS
PRE ECHOES	100	78	76
ION DENSITY FLUCTUATIONS	72	100	33
WIND CORNERS	80	30	100

Figure 7. Coincidence rates (in %) between the occurrence rate of PRE echoes, ion density fluctuations and wind corners obtained after a statistical analysis of the salvo launchings during MAP/WINE. One can see that, for example, 80% of the wind corners are associated with PRE echoes, while 33% of the ion density fluctuations are associated with wind corners.

GRAVITY WAVES

- GRAVITY WAVES CREATE CONVECTIVE INSTABILITIES IN PREFERENCE TO DYNAMIC INSTABILITIE FOR HIGH FREQUENCY WAVE MOTIONS

- LINEAR THEORY AND MONOCHROMATIC WAVES

- THE CRITERIUM FOR CONVECTIVE INSTABILITY IS:

$$\partial T/\partial z + \Gamma < 0 \qquad \text{OR} \qquad u' > c-U_0$$

WHERE

Γ IS THE ADIABATIC LAPSE RATE
u' IS THE HORIZONTAL PERTURBATION SPEED
c IS THE HORIZONTAL PHASE SPEED OF THE WAVE
U_0 IS THE MEAN WIND

THE INTRINSIC PHASE VELOCITY $c-U_0$ CAN BE FOUND FROM:

$$c-U_0 = (\omega_B/2\pi)\lambda_z$$

WHERE λ_z IS THE VERTICAL WAVELENGTH

Figure 8. Simple outline of the saturation mechanics for gravity waves.

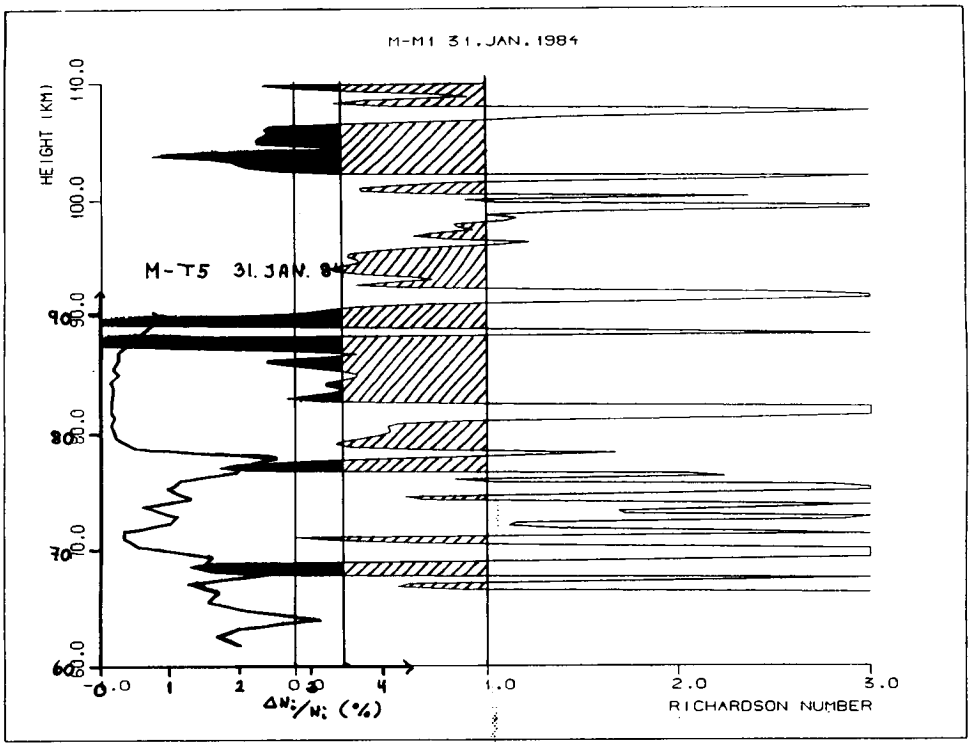

Figure 9. Comparison of Richardson numbers R_i derived from the active falling sphere M-M1 and ion density fluctuations $\Delta N_i/N_i$ (%) derived from the ion probe onboard M-T5 (31 Jan 1984). Good correlation between regions of convective instabilities and significant ion density fluctuations can be seen.

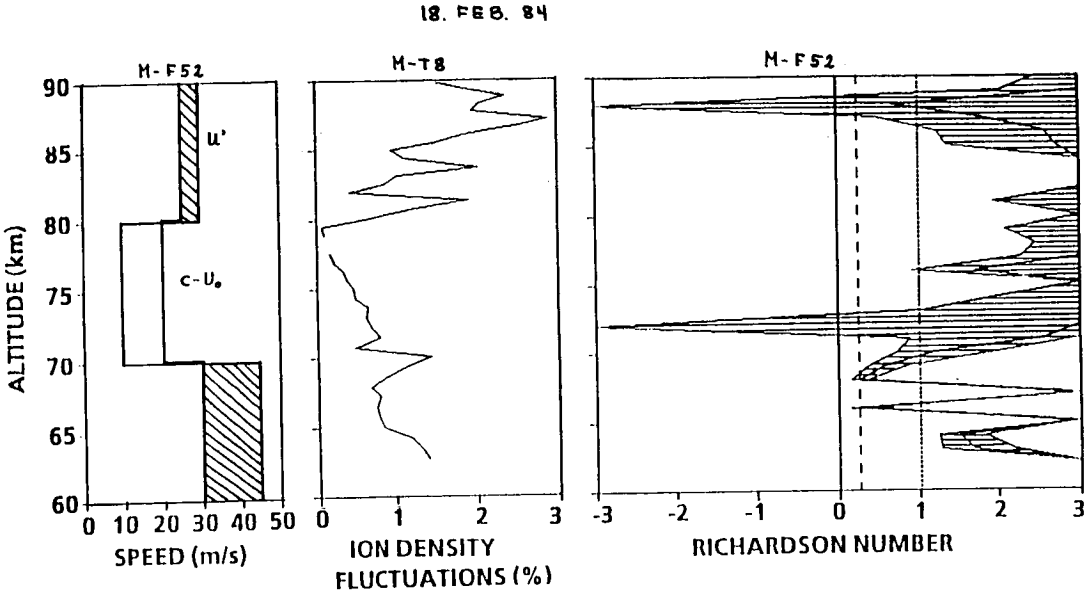

Figure 10. Case study of M-F52 and M-T8 (18 Feb 1984) showing the horizontal perturbation velocity u′ the intrinsic phase velocity c-**u**, ion density fluctuations and gradient Richardson number versus height. The hatched areas in the left-hand panel indicate those regions where u′ $\geq$ c – **u**. These regions correspond with regions of significant ion density fluctuations.

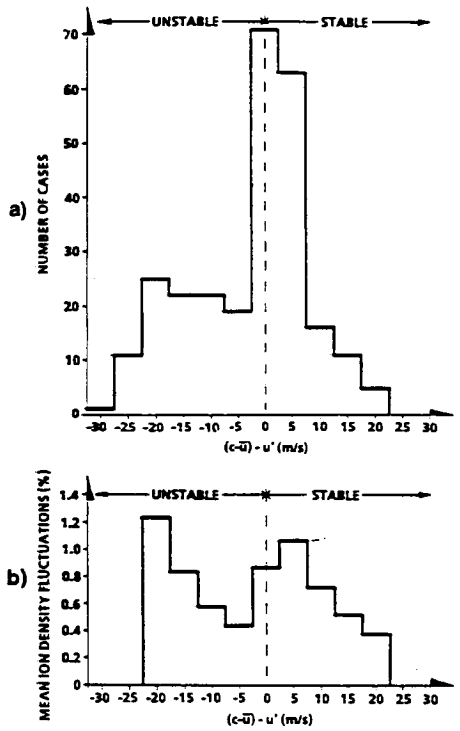

Figure 11. Results of a statistical investigation of the gravity wave saturation criteria ($d = (c - u_0) - u' \approx 0$) and turbulence. (a) Histogram showing number of cases as a function of d in intervals of 5 m/s. (b) Mean intensity of ion density fluctuations as a function of d.

CONCLUSIONS

- Previous disagreement between ε and K calculated using two different models have been explained.
- There is a minimum in turbulence at or below the mesopause region.
- There is a close relation between the extent of the intertial subrange, as determined by L_B and l_0, and the measured turbulence intensities.
- The wind and temperature fields derived from the meteorological rocket measurements have demonstrated that gravity waves are a dominant feature of the mesosphere in winter.
- Turbulent layers are associated with regions of convective and dynamic instabilities.
- The criterion for gravity wave saturation is often fulfilled in the high latitude winter mesosphere.
- There is a positive correspondence between strong turbulence and regions of radar echoes.
- Wind corners are predominantly associated with radar reflections (not with turbulence).